LASER MACROPOLISHING OF ADDITIVELY MANUFACTURED PARTS OF MARAGING STEEL WITH RESPECT TO SURFACE PROPERTIES

MARTIN BURES[1], MAX-JONATHAN KLEEFOOT[2], YUSUF BAKIR[1], MIROSLAV ZETEK[1]

[1]Regional Technological Institute, University of West Bohemia, Czech Republic

[2]Aalen University, Laser Application Centre, Germany

DOI: 10.17973/MMSJ.2022_10_2022125

mbures@rti.zcu.cz

This article is focused on the laser macro polishing of additively manufactured (AM) parts. The material that is being processed is maraging steel (MS1). The main part of the study is to find suitable parameters to significantly reduce the surface roughness of 3 surfaces with completely different topologies. The investigated parameters are scanning speed, defocussed laser and laser power. However, other material properties are also tested. Fatigue life, tensile and hardness testing were carried out for 3 different sets of laser macro polishing parameters. It was found that surface roughness reduction of Ra by over 90 % is possible. Interestingly, tensile testing of parameters 1 and 2 showed more brittle-like behaviour in comparison to parameter 3. This was further supported by hardness testing, which showed increased hardness in the centre of the samples.

KEYWORDS

Laser Polishing, Additive Manufacturing, Tensile testing, Fatigue testing, Hardness testing, Surface roughness, Maraging steel

1 INTRODUCTION

AM was invented in 1980, and thanks to advances in technology it has been possible to fully implement AM technology into industrial practice in recent years. In the beginning, AM was used mainly for rapid prototyping, however since 2016, increasingly parts have been created for end-use. Thanks to the ability to produce complex geometries and special structures for lightweight parts, there is a very high potential and motivation for the use of AM in industry. [Hollaender 2020].

One of the main problems of AM parts is the surface roughness due to the layer-by-layer building process. The main advantage of AM parts is that they can have complex geometries. AM parts usually exhibit high roughness surfaces, which has negative effect on the fatigue performance of the parts. Therefore, it is often required to post process these surfaces [Fuchs 2021]. Another problem is that complex AM parts exhibit different surface roughnesses because the surface roughness of AM parts depends significantly on build orientation, overhangs, support structures, and also variables such as printing parameters which can result in different surface roughnesses [Obilanade 2021]. However, even the measurement of the surface roughness can be a challenge. [Lee 2022] described that optical measurement (OM) or stylus-based measurement of AM surface roughness is not always feasible. OM is usually preferred when measuring surface roughness, however, especially when surface roughness reaches higher values, the pores and overhang structure on top of the surface can hinder standard measurement.

Postprocessing of the surface is often required to remove surface roughness and acquire precise geometries. Eliminating surface roughness is necessary to increase the fatigue life of a part. As-built specimens show worse fatigue behaviour than surface processed specimens. This low fatigue life derives from the surface roughness [Pegues 2018]. There are several studies that describe the fatigue life of as-built and postprocessed surfaces [Balachandramurthi 2018], [Vayssette 2018], [Sarkar 2019].

Laser polishing is an innovative approach to reducing surface roughness. Since laser macro polishing completely melts a layer, significant changes in microstructure and mechanical properties can be expected. [Chen 2020] studied the effects of laser polishing on AM surfaces. He found that a reduction of surface roughness by over 92 % was possible. Besides that, other material properties improved, such as microhardness due to grain refinement, corrosion resistance was increased, etc. However, laser polishing has one negative effect, and that is the tensile residual stress near the surface area as reported by [Tian 2018]. This could have a negative effect especially during the fatigue testing since cracking usually initiates at the surface. [Lee 2021] studied the effect of laser polishing on the fatigue performance of AM printed parts. Laser polished specimens showed better results than as-built ones in high cyclic regime (HCR), but showed similar or worse performance in lower cycle regime (LCR). The good performance in HCR was attributed to the reduction of surface roughness, and the bad performance in LCR was attributed to the tensile residual stress induced by laser polishing. After stress relief was applied, the laser polished specimens showed improved fatigue performance in LCR.

2 EXPERIMENTAL SETUP

2.1 Laser polishing device

Laser polishing was conducted using the processing machine Laser Cell TRUMPF TLC 40 (Figure 1) with a TRUMPF TruFiber 400 laser source with a maximum output power of 400W and wavelength of 1070 nm. This laser operates in a continuous wave regime, which means that the light is continuously pumped and emitted. However, the laser can be modulated and can produce pulse durations from µs up to long pulse durations. For guiding and focusing the laser beam on the workpiece a 2D PFO33 from TRUMPF with a focal length of 255 mm to focus the laser beam.

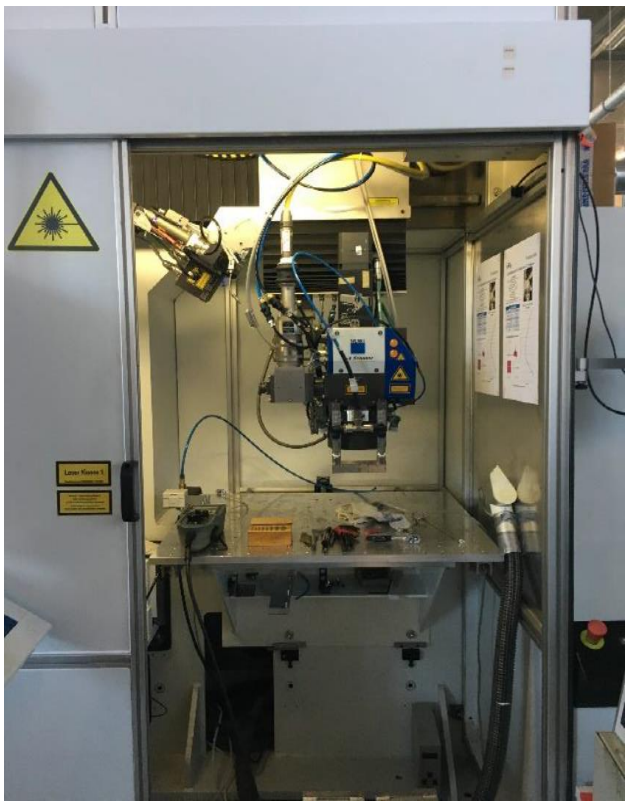

Figure 1 Laser cell used for laser polishing experiments

2.2 Processing chamber

The laser polishing was done in a processing chamber filled with argon, which served as a shielding gas. Shielding is necessary during laser polishing for two reasons. The first is to prevent the oxidation of the surface during laser polishing. The second is that oxygen amplifies the melting process. In Figure 2, the increased plasma plume/exotherm reaction during an unshielded polishing process is shown. This can potentially lead to optics damage. The amount of oxygen was measured using a PRO2 plus oxygen analyser of the company ORBITALSERVICE GmbH. The laser polishing process was started when the oxygen level inside the process chamber reached less than 40 ppm. The average oxygen level during the polishing was under 10 ppm.

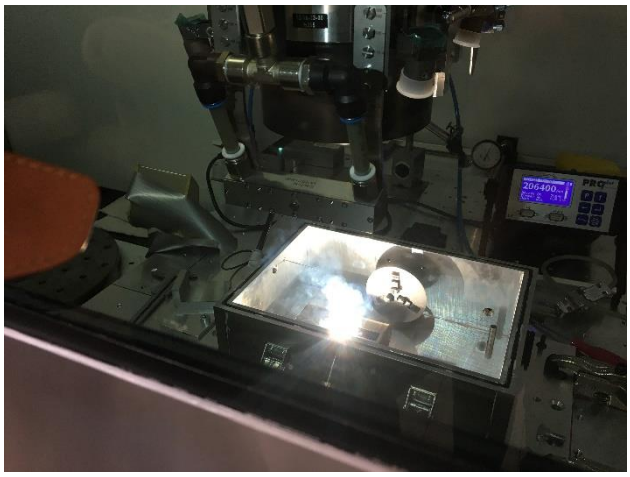

Figure 2 Processing chamber

2.3 Measuring laser spot diameter

The most frequently used laser beam shapes are Gaussian and Top Hat. The Gaussian beam shape has the highest laser intensity in the centre of the laser spot but intensity quickly decreases outwards from the centre of the spot. During laser polishing it is desirable to have a more even distribution of the laser intensity across the laser spot. This distribution can be achieved by defocussing. The defocussing was achieved by the movement of the optics away from the sample. Since a defocussed laser spot was used for this experiment, it was necessary to measure the laser spot diameter at different z heights so called caustic. In the focal plane, the laser spot diameter is 27.6 µm Figure 4.According to theory, the diameter in the 1 mm defocus should be 56 µm. Reality often differs from theory. The resulting focus diameter and divergence in reality always depend on the optical setup of the beam path. Among other things, these are influenced by aberrations and circular symmetry deviations. In the setup used, the measured M^2 is approx. 1.33 and the divergence angle in the far field is approx. 66 mrad. This results in a beam diameter of approx. 82 µm with a defocus of 1 mm. Near the focal plane we can observe that the shape of the caustic is non linear (waist) and slowly transitions to a more linear shape of caustic. Because it was necessary to obtain the diameter of the laser spot in higher z positions than were measured, we used the equation of the linear part (**Chyba! Nenalezen zdroj odkazů.**) of the caustic:

$$\omega = \frac{z + 0.1977}{0.0294} * 2 \qquad (1)$$

where ω is the laser spot diameter and z is the movement of the optics in relation to the focal plane. Thus we were able to calculate the laser spot diameter at any z position in relation to the focal plane.

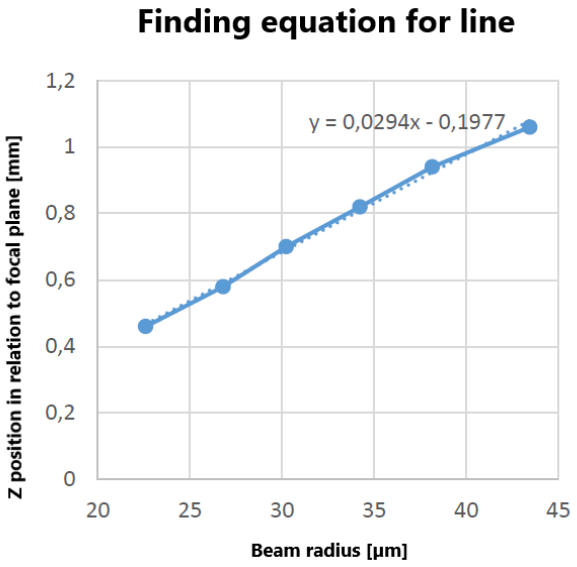

Figure 3 Equation for line to calculate laser spot diameter

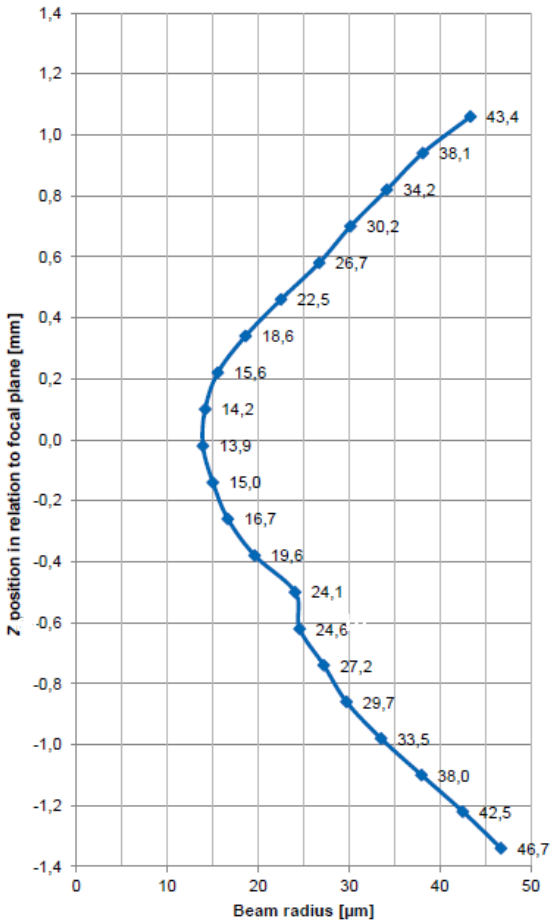

Figure 4 Measured caustic of the laser beam

2.4 Laser cleaning of the additive manufactured parts

Additively manufactured metal parts often need subsequent heat treatment (HT) to remove residual stress and homogenize their microstructure. On the surface of HT parts, there is a thin oxidation layer as well some powder trapped on the surface. Sandblasting is usually used to remove these impurities on the surface as well as enhancing the appearance of the part. However, sandblasting can result in a change to the surface topology, which is undesirable in this experiment. Therefore, laser cleaning was applied to remove the oxidation layer as well as the trapped powder. As can be seen in Figure 5 the top part is laser cleaned, and compared to the bottom part there is less powder visible on the surface. Laser cleaning of additively manufactured parts is strongly advised to reduce the chance of impurities occurring in the melted layers.

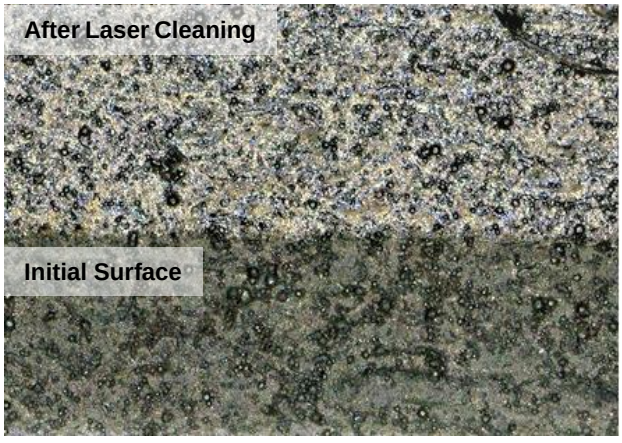

Figure 5 Effect of laser cleaning on powder particles

2.5 Material and Samples

The samples for laser polishing were manufactured by Direct Metal Laser Melting (DMLS) from MS1 powder, also known as 18% Ni Maraging 300, 1.2709 or X3NiCoMoTi 18-9-5. An EOS M290 machine was used to produce the samples using the default parameters obtained from the manufacturer.

Since surface roughness is highly dependent on the part orientation, the samples were printed with respect to the surface roughness. Three orientations were considered. The best surface quality is usually achieved when printing in the z direction with the surface perpendicular to the platform Figure 6 b). The second part was printed with an angle of 45 degrees Figure 6 a). This angle was chosen because it is considered as an angle that can be safely printed without using supports. However, surfaces printed at less than 45 degrees show very high surface roughness. The last sample is the top surface where upskin parameters are used Figure 6 c). This surface has a unique topology, because there is no staircase effect, which means that higher roughness is not caused by each layer but rather by each melt pool tracks.

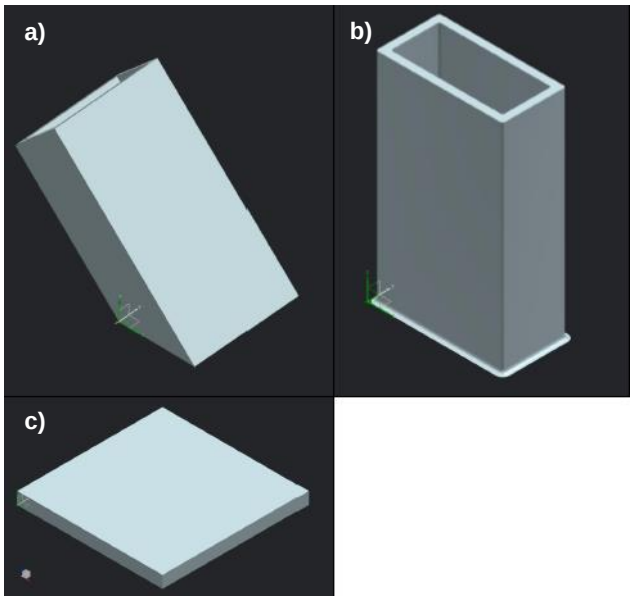

Figure 6 Samples printed for finding the parameters a) part printed under 45 degrees b) part printed in the Z direction c) top surface of the part printed in Z direction

To evaluate the effectivity of laser polishing, the reference surfaces had to be measured. The topology of 3 types of samples can be seen in Figures 7, 8 and 9. Figure 7 shows that the surface consists of each layer melted together with ball shape protrusions. These are partially melted particles on the part. Three measurements were conducted and the average for mean roughness Ra as well as the maximum roughness Rz was calculated. The measured results on the surface showed an Ra of Ra 6.12 µm and Rz 53.68 µm. The topology of the second measured surface which was printed at less than 45 degrees can be seen in **Chyba! Nenalezen zdroj odkazů.**. The colour range is much higher than in Figure 7 and no repeating pattern is visible. The reason for such a rough irregular surface is the mechanism of printing on the powder without supports. Each of the melt pools solidifies irregularly and together with a large amount of partially melted powder results in very high roughness. The measured roughness of Ra is 35.638 µm and Rz is 224.152 µm. It should be noted that these measurements were taken using an optical microscope and the very irregular surfaces can contain features which are not always visible using this technique. The last surface can be seen in Figure 9. As discussed above,

individual melt pool tracks can be seen in the picture. If Figure 7 and Figure 9 are compared, differences in topology can be seen. Figure 9 shows irregularities on the macro scale and large areas of valleys and peak surfaces are visible. This can cause problems for modulated continuous wave laser polishing, because the largest area that can be melted at one point is the laser spot diameter.

Ra [µm]	Rz [µm]
6.12	53.68

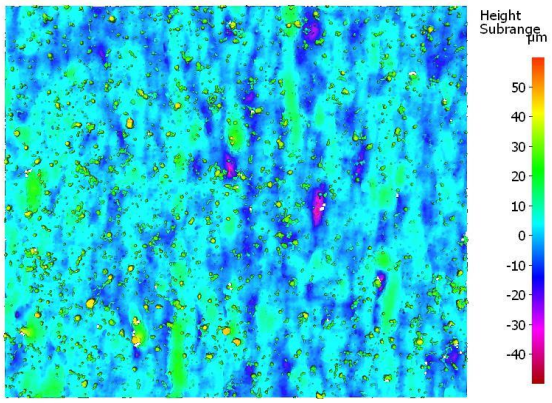

Figure 7 Topology and surface roughness values for surface printed in Z direction

Ra [µm]	Rz [µm]
35.64	226.15

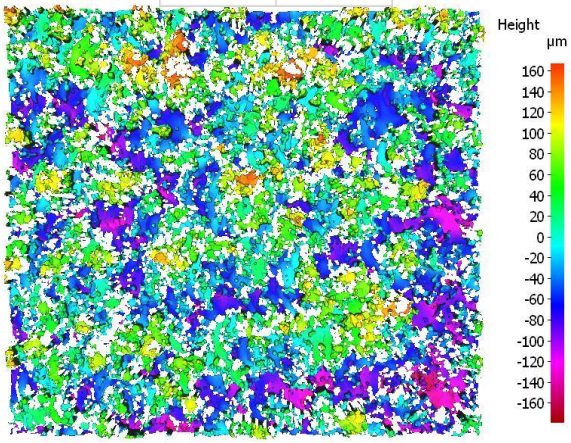

Figure 8 Topology and surface roughness values for a surface printed under 45 degrees

Ra [µm]	Rz [µm]
8	45.55

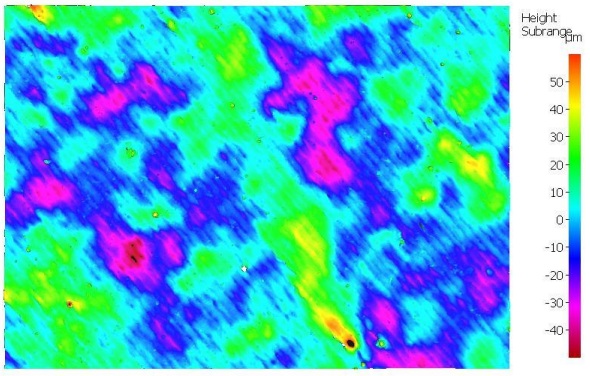

Figure 9 Topology and surface roughness values for a surface printed parallel with the platform

3 RESULTS AND DISCUSSION

3.1 Finding suitable parameters for a part printed in the Z direction in terms of surface roughness

The investigated parameters for laser polishing were laser power, scanning speed and focus position of the laser. Parameters such as pulse duration were kept constant. This study was conducted to observe the interaction of this type of laser with an AM surface and to get an idea of the influence of changing the parameters on the process of laser polishing. Surface roughness Ra was lower than 1 µm only when a pulse duration of 10 ms was applied. Therefore 10 ms was used for investigating the other parameters. Also, frequency was kept constant at a value of 94.56 Hz. This is the highest achievable value of frequency for this laser when a 10 ms pulse duration is chosen. Further lowering of the frequency value does not make sense, since decreasing the frequency will also result in lowering the laser speed for sufficient laser spot overlap, and this would result in significant overheating.

	Dependence of surface roughness on distance from focal plane		
Distance from focal plane [mm]	Calculated laser spot diameter [µm]	Measured surface roughness	
		Ra [µm]	Rz [µm]
9	626	0.711	8.405
10	694	0.722	17.79
11	762	0.826	10.36
12	830	0.746	10.39
13	898	0.777	7.739
14	966	0.712	4.691
15	1034	0.794	8.342

Table 1 The dependency of surface roughness on a defocused laser beam for a part printed in the Z direction

Table 1 shows the influence of a defocused laser on surface roughness. The minimum distance from the focal plane was 9 mm. This parameter was not chosen randomly. When we set up the laser defocus at less than 9 mm, the glass part of the processing chamber was influenced. Based on the results from Table 1 it can be seen that a defocus greater than 9 mm did not have a significant effect on the surface roughness. However, a certain defocus had to be chosen, therefore a defocus of 14 mm was chosen based on the best Ra and Rz parameters.

Dependence of surface roughness on power and its influence on pulse energy				
Power [W]	Energy of pulse [J]	Laser Intensity I [W/mm^2]	Ra [µm]	Rz [µm]
350	3.5	478	0.951	9.446
325	3.25	444	1.056	14.02
300	3	409	0.679	15.1
275	2.75	375	0.722	12.352
250	2.5	341	0.715	10.32
225	2.25	307	0.807	7.961
200	2	273	0.768	8.267

Table 2 The dependency of surface roughness on power for a part printed in the Z direction

Another parameter whose influence on surface roughness was observed is power. As can be seen in Table 2, only the parameters with power of 325 W and 350 W showed higher values of surface roughness. Other parameters showed similar results. The power in this range did not show a significant influence on the surface roughness.

Dependence of roughness on changes to scanning speed and its influence on spot overlap			
Scanning speed [mm/s]	Spot overlap [%]	Ra [µm]	Rz [µm]
5	94	0.785	7.935
10	88	0.595	7.846
15	82	0.65	15.49
20	76	0.614	12.16
25	70	0.741	8.308

Table 3 The dependency of surface roughness on scanning speed for a part printed in the Z direction

In Table 3 we can see the results of surface roughness based on scanning speed. Scanning speed has, together with frequency, an influence on the spot overlap. Small changes can be seen between the roughness values for different speeds. The scanning speed of 10 mm/s showed the most promising results. The initial roughness of Ra 6.12 µm was reduced to Ra of 0.595 µm, which is a reduction of surface roughness by 90%.

3.2 Finding suitable parameters for a surface printed under 45 degrees in terms of surface roughness

Dependency of surface roughness on laser power				
Power [W]	Energy of pulse [J]	Laser Intensity I [W/mm^2]	Ra [µm]	Rz [µm]
400	4	546	1.538	13.17
375	3.75	512	1.333	14.67
350	3.5	478	1.742	20.46
325	3.25	444	1.598	22.59
300	3	409	1.944	25.7
275	2.75	375	2.056	19.19
250	2.5	341	2.608	22.65
225	2.25	307	2.049	14.78

Table 4 The dependency of surface roughness on power for a surface printed under 45 degrees

As before, changes to power and speed were applied. Since different distances from the focal plane have a very similar effect on the resulting surface roughness, a defocus of 14 mm was also chosen here. It was found that increased power results in decreased surface roughness.

Roughness dependency on changed speed and its influence on spot overlap			
Speed [mm/s]	Spot overlap [%]	Ra [µm]	Rz [µm]
5	94	1.376	27.85
10	88	1.474	15.47
15	82	1.247	40.07
20	76	1.365	20.33
25	70	1.614	17.44

Table 5 The dependency of surface roughness on scanning speed for a surface printed under 45 degrees

The last parameter was again scanning speed, which has an effect on spot overlap. The best roughness of Ra was achieved with speed of 15 mm/s. The final acquired roughness was 1.247 µm and total reduction of surface roughness by 96% was achieved.

3.3 Finding suitable parameters for a surface printed parallel with the platform in terms of surface roughness

	Dependency of surface roughness on power and its influence on pulse energy			
Power [W]	Energy of pulse [J]	Laser Intensity I [W/mm^2]	Ra [µm]	Rz [µm]
350	3.50	478	0.88	20.72
325	3.25	444	0.963	21.38
300	3.00	409	1.022	14.29
275	2.75	375	0.99	14.12
250	2.50	341	1.105	16.8
225	2.25	307	0.95	22.89
200	2.00	273	0.946	21.76

Table 6 The dependency of surface roughness on power for a surface printed parallel with the platform

The last surface where laser polishing was applied is the top surface of the part in Figure 6 c). This surface is unique in comparison to the others, because this surface does not exhibit the staircase effect, so it should show the lowest roughness. However, in Figure 9 it is visible that there is a non-homogenous surface topology on the macro scale. This could have a significant effect on the resulting surface roughness. When different power was applied, we can see that the resulting surface roughness showed higher values then the part printed in the Z direction. The resulting higher roughness might be caused by the macro scale unevenness. Since the used laser operates in a modulated regime, after every pulse the melt pool gets solidified. So only the area of the laser spot can be polished, therefore large uneven areas can result in insufficient polishing. As can be seen in Table 6, the results again showed similar results.

Roughness dependency on changed speed and its influence on spot overlap			
Speed [mm/s]	Spot overlap [%]	Ra [µm]	Rz [µm]
5	94	0.993	5.317
10	88	0.978	10.78
15	82	0.78	11.73
20	76	0.759	10.14
25	70	0.85	8.467

Table 7 The dependency of surface roughness on scanning speed for a surface printed parallel with the platform

In contrast to power, different scanning speeds showed some changes in the surface roughness. Speeds of 15 mm/s and 20 mm/s produce the best surface roughness at a value of around Ra 0.7 µm. Percentage-wise the reduction of roughness from the as-built state is around 90.5 %.

3.4 Fatigue test

The optimized parameters were applied to the fatigue test samples. However, another problem emerged. Since the scanned area was small (15x15 mm), overheating was not observed during the parameter testing. Nevertheless, when applied to the fatigue samples, the large surface area with a small cross-section caused severe overheating and the sample was deformed. Since all the test parameters were found in terms of the lowest roughness, it would not be feasible to find completely new parameters, therefore changes needed to be made.

Parameter number	Power [W]	Speed [mm/s]	Frequency [Hz]	Pulse duration [ms]
1	110	10	93	10
2	300	10	93	5
3	350	50	500	1.3

Table 8 List of parameters used for fatigue, tensile and hardness for a surface printed parallel with the platform

For the first parameter only, the laser power was reduced. It was found that changing the laser power had no significant effect on the resulting surface roughness. Therefore, lower power was applied to reduce the surface roughness, but at the same time reducing the overheating of the part so no deformation occurs. Therefore, 110 W was applied for the first parameters. The other parameters were set up to correlate with each other in terms of laser energy. Between parameters 1 and 2, you can see that speed and frequency were kept constant, but the power and pulse duration were changed to keep a similar laser energy per pulse as the first one so we can correlate them. Parameter 3 was a trial parameter to achieve the least overheating.

Fatigue testing is expensive and time demanding, therefore each parameter was applied to three samples, and they were tested to compare their fatigue behaviour at certain stress amplitude and not to get an S-N curve.

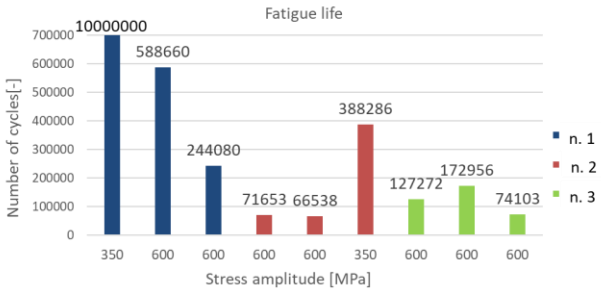

Graph 1 Comparing fatigue life of 3 laser polishing parameters

The first stress amplitude of 350 MPa was chosen. The material at such a relatively low stress amplitude could be utilized to investigate rapture due to the flaws within the material. Since at lower values of stress/strain amplitude the main governing mechanism for rapture is the crack initiation. [Lee 2022] These flaws could be formed as a result of overheating, therefore this lower value of stress amplitude was set. The first tested parameter was parameter n. 2. As can be seen, the sample failed at 388286 cycles. However, when parameter n. 1 was tested, the samples resulted in runout. Since it was necessary to have samples that result in crack failure, the tested stress amplitude was increased to 600 MPa for the rest of the samples. As can be seen in Graph 1, the best result was achieved with parameter n. 1.

3.5 Tensile test

In figures 10 to 12 we can see the effects of laser polishing on the tensile samples.

Figure 10 Tensile sample polished using parameter 1

Figure 11 Tensile sample polished using parameter 2

Figure 12 Tensile sample polished using parameter 3

Parameter number	Number of the sample	Yield strength $Rp_{0,2}$ [MPa]	Tensile strength Rm [MPa]	Ductility A [%]
1	7	1297	1362	0.9
	8	1337	1338	0.7
	9	1277	1297	1.2
2	6	1340	1354	0.3
	14	1341	1350	0.9
3	10	889	1137	11.8
	11	884	1131	11.5

Table 9 Results of tensile testing

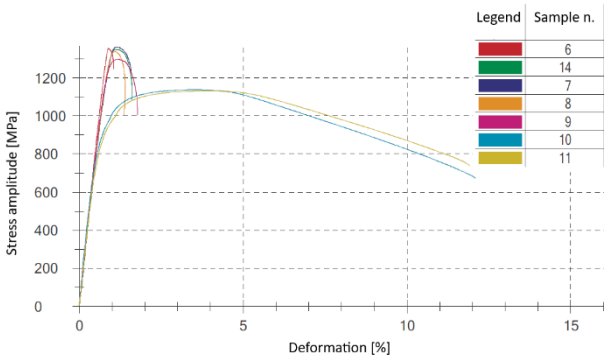

Graph 2 Stress strain curve of tensile test

In the Table 9 and Graph 2, we can see significant differences between parameter 3 and parameters 1 and 2 from the tensile properties according to the manufacturer which are: Rp 0.2: 870 ± 100 [MPa], Rm: 1100 ± 100 [MPa] a A: 12 ± 4 [%]. Parameter number 3 is within the limits of the values given by the manufacturer. However, the parameters behave completely differently. They have higher tensile strength. Also, with parameters 1 and 2 we can see that yield strength and ultimate strength are almost identical, which indicates brittle behaviour. Unfortunately, the ductility could not be measured, because the part cracked outside the sensors range (values in the Table 9 in red colour). However, all the samples were heat treated, therefore the material/mechanical changes must have occurred during the laser polishing process. Therefore, hardness of the samples was measured.

3.6 Hardness tests

The tensile sample was cut across the specimen for hardness measurement. Then several hardness measurements were performed according to the Vickers test. A preload of HV10 was used for indenting. Each indentation was done in 1 mm steps across the cross-section and hardness was measured.

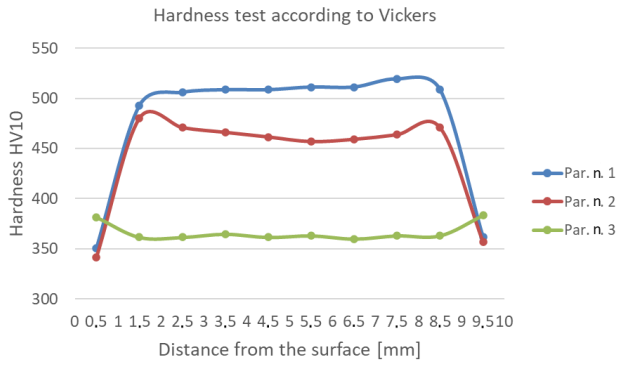

Graph 3 Results of hardness test according to HV10

As can be seen in Graph 3, parameters 1 and 2 show the greatest hardness. Also, we can see that for parameters 1 and 2 the lowest roughness is achieved near the surface and there is a steep increase in the hardness near the centre. This was unexpected, because the most significant changes were anticipated in the subsurface area, because that is where melting occurred. Therefore, we must conduct an investigation to find out what initiated this hardening process in the middle of the part. An indication might be that material MS1 is called maraging steel, which means that aging is the main process of hardening. The accumulated heat during the laser polishing is a probable cause for the aging process that occurred in these parts. The largest overheating was observed when laser polishing with parameters 1 and 2 were applied on the parts. Parameter 3 was least overheated in comparison with other parameters. This corresponds with the set process parameters. Parameters 1 and 2 were set with longer pulse duration, therefore more interaction time between the laser and the substrate, which led to the higher amount of heat accumulated within the part. Scanning speed was also set lower in parameter 1 and 2 in comparison to parameter 3, which contributed to the heat accumulation within the samples. This corresponds to the results shown in Graph 3.

4 CONCLUSIONS

Laser polishing was applied to surfaces that were printed at different angles. AM parts have different surface roughnesses depending on their surface orientation and the staircase effect. In this work, surface roughnesses from Ra 6 to 35 µm were measured. The influence of basic laser parameters such as the distance from the focal plane, laser power and laser speed were investigated. Also, preliminary investigation of mechanical properties such as tensile testing, fatigue testing and hardness testing were performed on the samples with laser polished surfaces.

1. Laser polishing showed promising results in terms of surface roughness reduction. It was observed that a reduction of surface roughness of over 90 % was achieved on all three surfaces. The best surface roughness was achieved with surfaces printed in the Z direction. A final roughness of Ra 0.596 µm was achieved. It was observed that in the range we investigated neither defocusing, laser power, nor speed had a significant effect on the surface roughness. Therefore, it is assumed that pulse duration had the biggest effect on surface roughness.
2. Fatigue testing samples showed interesting behaviour. The best results were achieved with parameter 1. This parameter was found after a series of tests done, due to severe overheating, at a reduced power of 110 W. However, to properly investigate fatigue life more samples will have to be tested to form an S-N curve. However, this preliminary testing showed that parameters 2 and 3 are not suitable in terms of fatigue life.
3. Tensile testing gave us an idea of the material changes that occurred during laser polishing. Parameter 3 has shown similar behaviour to standard AM samples. Since parameters 1 and 2 showed similar yield and tensile strength which indicates brittle-like behaviour, it was decided to perform hardness testing to confirm this behaviour.
4. Hardness testing showed that parameters 1 and 2 exhibited the highest values of hardness according to Vickers. These samples showed the greatest overheating as they had the longest pulse duration and a slow scanning speed. Because of these process parameters the heat accumulated within the parts. Therefore, it is assumed that the age hardening process began and precipitation hardening occurred. Another indication is that parameter set 3 did not cause the sample to overheat and the part was not hardened.

As can be seen from the results, laser polishing shows promising results in terms of surface roughness reduction, however since parameter finding focused solely on surface roughness reduction, other undesirable effects will not be apparent until

the parameters are applied to the samples. The overheating caused significant problems during laser polishing. Therefore, it might be desirable to investigate shorter pulse durations, to give a wider parameter range of frequencies and speeds to reduce the polishing time, which will decrease overheating.

ACKNOWLEDGMENTS

The work was supported from ERDF "Research of additive technologies for future applications in machinery industry - RTI plus" (No. CZ.02.1.01/0.0/0.0/18_069/0010040).

REFERENCES

[Balachandramurthi 2018] Balachandramurthi, A.R., Moverare, J., Dixit, N., Pederson, R., 2018. Influence of defects and as-built surface roughness on fatigue properties of additively manufactured Alloy 718. Materials Science and Engineering: A 735, 463–474. https://doi.org/10.1016/j.msea.2018.08.072

[Chen 2020] Chen, L., Richter, B., Zhang, X., Ren, X., Pfefferkorn, F.E., 2020. Modification of surface characteristics and electrochemical corrosion behavior of laser powder bed fused stainless-steel 316L after laser polishing. Additive Manufacturing 32, 101013. https://doi.org/10.1016/j.addma.2019.101013

[Fuchs 2021] C. Fuchs, L. Kick, O. Leprevost, M. F. Zaeh, Assessment of finish machining and mass finishing as post-processing methods for PBF-LB/M-Manufactured 316L, MM Sci. J. March (2021) 5187-5194.

[Hollaender 2020] Hollaender, Andreas, a Patrick Cosemans. 2020. „Surface technology for additive manufacturing". Plasma Processes and Polymers 17(1):1900155. doi: 10.1002/ppap.201900155.

[Lee 2021] Lee, S., Ahmadi, Z., Pegues, J.W., Mahjouri-Samani, M., Shamsaei, N., 2021. Laser polishing for improving fatigue performance of additive manufactured Ti-6Al-4V parts. Optics & Laser Technology 134, 106639. https://doi.org/10.1016/j.optlastec.2020.106639

[Lee 2022] Lee, S., Shao, S., Wells, D.N., Zetek, M., Kepka, M., Shamsaei, N., 2022. Fatigue behavior and modeling of additively manufactured IN718: The effect of surface treatments and surface measurement techniques. Journal of Materials Processing Technology 302, 117475. https://doi.org/10.1016/j.jmatprotec.2021.117475

[Obilanade 2021] Obilanade, D., Dordlofva, C., & Törlind, P. (2021). SURFACE ROUGHNESS CONSIDERATIONS IN DESIGN FOR ADDITIVE MANUFACTURING - A LITERATURE REVIEW. Proceedings of the Design Society, 1, 2841–2850. Cambridge Core. https://doi.org/10.1017/pds.2021.545

[Pegues 2018] Pegues, J., Roach, M., Scott Williamson, R., Shamsaei, N., 2018. Surface roughness effects on the fatigue strength of additively manufactured Ti-6Al-4V. International Journal of Fatigue 116, 543–552. https://doi.org/10.1016/j.ijfatigue.2018.07.013

[Sarkar 2019] Sarkar, S., Kumar, C.S., Nath, A.K., 2019. Effects of different surface modifications on the fatigue life of selective laser melted 15–5 PH stainless steel. Materials Science and Engineering: A 762, 138109. https://doi.org/10.1016/j.msea.2019.138109

[Tian 2018] Tian, Y., Gora, W.S., Cabo, A.P., Parimi, L.L., Hand, D.P., Tammas-Williams, S., Prangnell, P.B., 2018. Material interactions in laser polishing powder bed additive manufactured Ti6Al4V components. Additive Manufacturing 20, 11–22. https://doi.org/10.1016/j.addma.2017.12.010

[Vayssette 2018] Vayssette, B., Saintier, N., Brugger, C., Elmay, M., Pessard, E., 2018. Surface roughness of Ti-6Al-4V parts obtained by SLM and EBM: Effect on the High Cycle Fatigue life. Procedia Engineering 213, 89–97. https://doi.org/10.1016/j.proeng.2018.02.010

CONTACTS:

Ing. Martin Bures
Regional Technological Institute
University of West Bohemia
Univerzitni 8, Pilsen 301 00, Czech Republic
Tel.: +420 377638788
e-mail: mbures@rti.zcu.cz
www.zcu.cz